



Fading performance evaluation of a semi-blind adaptive space–time equaliser for frequency selective MIMO systems

Huiting Cheng^a, Sheng Chen^{b,c,*}

^a*Advanced Wireless Communication Research Center, University of Electro-Communications, Tokyo 182-8585, Japan*

^b*Electronics and Computer Science, Faculty of Physical and Applied Science, University of Southampton, Southampton SO17 1BJ, UK*

^c*Faculty of Engineering, King Abdulaziz University, Jeddah 21589, Saudi Arabia*

Received 8 January 2010; received in revised form 7 May 2010; accepted 6 September 2011

Available online 17 September 2011

Abstract

A semi-blind adaptive space–time equaliser (STE) has recently been proposed based on a concurrent gradient-Newton (GN) constant modulus algorithm (CMA) and soft decision-directed (SDD) scheme for dispersive multiple-input multiple-output (MIMO) systems that employ high-throughput quadrature amplitude modulation signalling. A minimum number of training symbols, approximately equal to the dimension of the STE, is used to provide a rough initial estimate of the STE's weight vector. The concurrent GN based CMA and SDD blind adaptive scheme is then adopted to adapt the STE. This semi-blind STE has a complexity similar to that of the training-based recursive least squares (RLS) algorithm. For stationary MIMO channels, it has been demonstrated that this semi-blind adaptive STE is capable of converging fast to the optimal minimum mean square error STE solution. In this contribution, we investigate the performance of this semi-blind adaptive STE operating in Rayleigh fading MIMO systems. Our results obtained show that the tracking performance of this semi-blind adaptive algorithm is close to that of the training-based RLS algorithm. Thus, this semi-blind adaptive STE offers an effective and practical means to successfully operate under the highly dispersive and fading MIMO environment.

© 2011 The Franklin Institute. Published by Elsevier Ltd. All rights reserved.

*Corresponding author at: Electronics and Computer Science, Faculty of Physical and Applied Science, University of Southampton, Southampton SO17 1BJ, UK.

E-mail addresses: hct@awcc.uec.jp (H. Cheng), sqc@ecs.soton.ac.uk (S. Chen).

1. Introduction

Multiple-input multiple-output (MIMO) techniques are capable of offering a high channel capacity in interference-free scenarios, albeit their achievable performance is limited by the multi-user interference. For frequency selective MIMO systems, space–time equalisers (STEs) [1–18] offer an effective means of suppressing both intersymbol interference and co-channel interference at the receiver. For the sake of further improving the achievable bandwidth efficiency, high-throughput quadrature amplitude modulation (QAM) schemes [19] have become popular in numerous wireless network standards. For example, the 16-QAM and 64-QAM schemes were adopted in the recent WiMAX standard [20]. Adaptive implementation of STE can be realised using training based adaptive algorithms, such as the recursive least squares (RLS) algorithm [21]. However, a large number of training symbols is required to properly train a STE, which considerably reduces the achievable system throughput. Note that under a dispersive MIMO environment, the STE's input signal is highly correlated, and stochastic-gradient (SG) based adaptive algorithms, such as the training-based least mean square (LMS) algorithm, suffer seriously from slow convergence and high steady-state misadjustment [21].

Blind adaptive methods do not require training symbols and, therefore, do not reduce the achievable system throughput. However, pure blind adaptive STEs typically require excessively high complexity and suffer from very slow convergence. Moreover, blind methods result in unavoidable estimation and decision ambiguities [22,23]. An effective means of resolving the estimation and decision ambiguities of blind adaptive methods is to employ a few training symbols, and this leads to attractive semi-blind schemes. Many SG-based semi-blind methods [24–30] have been proposed for frequency nonselective MIMO systems. In particular, the work of [30] developed a SG-based concurrent constant modulus algorithm (CMA) and soft decision-directed (SDD) scheme for narrowband MIMO systems that employ high-order QAM signalling. In this semi-blind method, a few training symbols, approximately equal to the dimension of the spatial equaliser, are first used to provide a rough least squares (LS) estimate of the spatial equaliser's weight vector. The SG based CMA and SDD scheme, originally developed for blind equalisation of single-input single-output systems [31,32], is then employed to adapt the spatial equaliser. This semi-blind SG based scheme converges fast to the minimum mean square error (MMSE) spatial equalisation solution, with a complexity similar to that of the training-based LMS algorithm. A SG-based semi-blind adaptive scheme however suffers from slow convergence and high steady-state misadjustment, when operating in frequency selective MIMO systems.

Recently, a gradient-Newton (GN) based semi-blind concurrent CMA and SDD algorithm [33] was proposed to adapt the STE that operates in wideband MIMO systems. GN-type algorithms [34,35] employ the inverse of the input signal's autocorrelation matrix to modify stochastic gradient, which results in much faster convergence than SG-type algorithms in highly correlated signal environments. The inverse of the autocorrelation matrix is implemented in the same way as in the RLS algorithm [21]. The complexity of a GN-based adaptive algorithm is therefore similar to that of the RLS algorithm. For stationary dispersive MIMO systems, the results reported in [33] have demonstrated that this semi-blind GN-CMA+SDD based STE is capable of converging fast to the optimal MMSE STE solution and its convergence speed is very close to that of the training-based RLS algorithm. No result however has been produced to date for this semi-blind

GN-CMA+SDD based STE operating in time-varying MIMO channels. The contribution of this paper is that we investigate the tracking performance of this semi-blind adaptive STE operating in dispersive Rayleigh fading MIMO systems. Our results obtained show that the tracking performance and the symbol error rate (SER) of this semi-blind adaptive STE are close to those of the continuously training-based RLS STE. These results are very significant, because the continuously training-based RLS STE is impossible to realise and its SER offers a low bound of the system’s achievable performance. This study thus demonstrates that the semi-blind GN-CMA+SDD based algorithm offers an efficient and practical means to adapt a STE in the hostile dispersive fading MIMO environment.

2. System model and STE structure

We consider the space-division multiple-access (SDMA) induced MIMO system as depicted in Fig. 1, where each of the Q users is equipped with a single transmit antenna and the receiver is assisted by a P -element antenna array. We point out that this structure is equally applicable to a single-user Q -layered spatial multiplexing based MIMO system. Denote the symbol-rate channel impulse response (CIR) connecting the q th transmit antenna to the p th receive antenna at the symbol index k as

$$\mathbf{c}_{p,q}(k) = [c_{0,p,q}(k) \ c_{1,p,q}(k) \ \cdots \ c_{n_c-1,p,q}(k)]^T, \tag{1}$$

where without loss of generality we have assumed that each of the $P \times Q$ CIRs has the same length of n_c . Magnitudes of the CIR taps are uncorrelated Rayleigh processes, and each CIR tap has a root mean power of $\sqrt{0.5} + j\sqrt{0.5}$. The normalised Doppler frequency of the system is denoted by f_d , and continuously fluctuating fading is assumed, which provides a different fading magnitude and phase for each CIR tap $c_{i,p,q}$ at each k .

The symbol-rate received signal samples $x_p(k)$, for $1 \leq p \leq P$, can be expressed as [36,37]

$$x_p(k) = \sum_{q=1}^Q \sum_{i=0}^{n_c-1} c_{i,p,q}(k) s_q(k-i) + n_p(k), \tag{2}$$

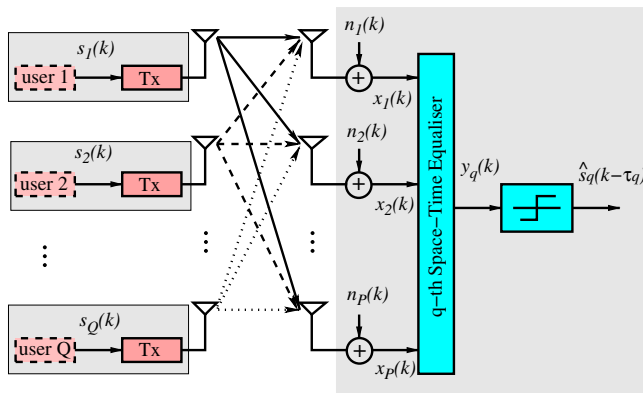


Fig. 1. SDMA induced MIMO system, where each of the Q users is equipped with a single transmit antenna and the receiver is assisted by a P -element antenna array.

where $n_p(k)$ is a complex-valued Gaussian white noise process with $E[|n_p(k)|^2] = 2\sigma_n^2$, $s_q(k)$ is the k th transmitted symbol of user q with the symbol energy $E[|s_q(k)|^2] = \sigma_s^2$, and $s_q(k)$ takes the values from the M -QAM symbol set

$$\mathcal{S} \triangleq \{s_{i,l} = u_i + ju_l, 1 \leq i, l \leq \sqrt{M}\} \tag{3}$$

with the real-part symbol $\Re[s_{i,l}] = u_i = 2i - \sqrt{M} - 1$ and the imaginary-part symbol $\Im[s_{i,l}] = u_l = 2l - \sqrt{M} - 1$. The average signal-to-noise ratio (SNR) of the system is defined as

$$\text{SNR} = \frac{\sum_{q=1}^Q \sum_{p=1}^P E[\mathbf{c}_{p,q}^H(k) \mathbf{c}_{p,q}(k)] \sigma_s^2}{2QP\sigma_n^2} = \frac{n_C \sigma_s^2}{2\sigma_n^2}. \tag{4}$$

The STE for detecting the q th user’s data is depicted in Fig. 2. The q th STE’s output, given by

$$y_q(k) = \sum_{p=1}^P \sum_{i=0}^{D-1} w_{i,p,q}^*(k) x_p(k-i), \tag{5}$$

is passed to the decision device to produce an estimate $\hat{s}_q(k - \tau_q)$ of the transmitted symbol $s_q(k - \tau_q)$, where D is the temporal filter’s length, $w_{i,p,q}(k)$ are the weights of the STE at the symbol index k , and $0 \leq \tau_q \leq D + n_C - 2$ is the decision delay.

Define the overall received signal vector $\mathbf{x}(k) = [\mathbf{x}_1^T(k) \ \mathbf{x}_2^T(k) \ \dots \ \mathbf{x}_P^T(k)]^T$, where

$$\mathbf{x}_p(k) = [x_p(k) \ x_p(k-1) \ \dots \ x_p(k-D+1)]^T, \tag{6}$$

for $1 \leq p \leq P$. Then $\mathbf{x}(k)$ can be expressed by the well-known MIMO model

$$\mathbf{x}(k) = \mathbf{C}(k)\mathbf{s}(k) + \mathbf{n}(k), \tag{7}$$

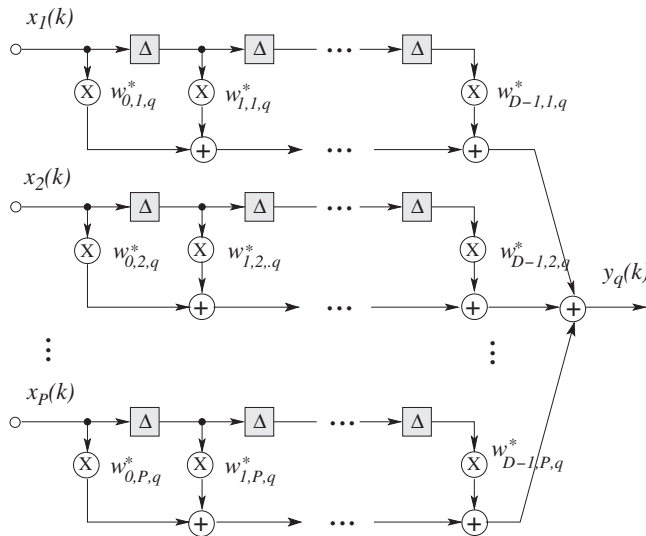


Fig. 2. Space–time equaliser for user q , where Δ denotes the symbol-spaced delay, P is the number of receive antennas, D denotes the length of temporal filter, and $1 \leq q \leq Q$ with Q being the number of users.

where $\mathbf{n}(k) = [\mathbf{n}_1^T(k) \mathbf{n}_2^T(k) \cdots \mathbf{n}_P^T(k)]^T$ with

$$\mathbf{n}_p(k) = [n_p(k) \ n_p(k-1) \cdots n_p(k-D+1)]^T, \tag{8}$$

for $1 \leq p \leq P$, the transmitted symbol vector of all the users $\mathbf{s}(k) = [\mathbf{s}_1^T(k) \ \mathbf{s}_2^T(k) \cdots \mathbf{s}_Q^T(k)]^T$ with

$$\mathbf{s}_q(k) = [s_q(k) \ s_q(k-1) \cdots s_q(k-D-n_C+2)]^T, \tag{9}$$

for $1 \leq q \leq Q$, and the overall system's CIR matrix at the symbol index k

$$\mathbf{C}(k) = \begin{bmatrix} \mathbf{C}_{1,1}(k) & \mathbf{C}_{1,2}(k) & \cdots & \mathbf{C}_{1,Q}(k) \\ \mathbf{C}_{2,1}(k) & \mathbf{C}_{2,2}(k) & \cdots & \mathbf{C}_{2,Q}(k) \\ \vdots & \vdots & \cdots & \vdots \\ \mathbf{C}_{P,1}(k) & \mathbf{C}_{P,2}(k) & \cdots & \mathbf{C}_{P,Q}(k) \end{bmatrix}, \tag{10}$$

with the $D \times (D + n_C - 1)$ CIR matrix associated with the user q and the receive antenna p given by the Toeplitz form

$$\mathbf{C}_{p,q}(k) = \begin{bmatrix} \mathbf{c}_{p,q}^T(k) & 0 & \cdots & 0 \\ 0 & \mathbf{c}_{p,q}^T(k) & \ddots & \vdots \\ \vdots & \ddots & \ddots & 0 \\ 0 & \cdots & 0 & \mathbf{c}_{p,q}^T(k) \end{bmatrix} \tag{11}$$

for $1 \leq p \leq P$ and $1 \leq q \leq Q$. Similarly, the STE for detecting the q th user's data can be expressed as

$$y_q(k) = \mathbf{w}_q^H(k) \mathbf{x}(k) \tag{12}$$

where the weight vector of the q th STE at k is given by $\mathbf{w}_q(k) = [\mathbf{w}_{1,q}^T(k) \ \mathbf{w}_{2,q}^T(k) \cdots \mathbf{w}_{P,q}^T(k)]^T$ with

$$\mathbf{w}_{p,q}(k) = [w_{0,p,q}(k) \ w_{1,p,q}(k) \cdots w_{D-1,p,q}(k)]^T. \tag{13}$$

The dimension of the STE is therefore $N_{\text{STE}} = P \cdot D$.

The mean square error (MSE) value for the STE of Eq. (12) with the weight vector $\mathbf{w}_q(k)$ can be expressed by

$$J_{\text{MSE}}(\mathbf{w}_q(k), k) = \sigma_s^2 (1 - \mathbf{w}_q^H(k) \mathbf{C}_{|q_\eta}(k) - \mathbf{w}_q^T(k) \mathbf{C}_{|q_\eta}^*(k)) + \sigma_s^2 \mathbf{w}_q^H(k) \left(\mathbf{C}(k) \mathbf{C}^H(k) + \frac{2\sigma_n^2}{\sigma_s^2} \mathbf{I} \right) \mathbf{w}_q(k), \tag{14}$$

where \mathbf{I} denotes the $N_{\text{STE}} \times N_{\text{STE}}$ dimensional identity matrix, $q_\eta = (q-1)(D + n_C - 1) + (\tau_q + 1)$ and $\mathbf{C}_{|i}$ the i th column of \mathbf{C} . Then the average MSE

$$J_{\text{AMSE}}(\mathbf{W}(k), k) = \frac{1}{Q} \sum_{q=1}^Q J_{\text{MSE}}(\mathbf{w}_q(k), k), \tag{15}$$

over all the Q users can be used to investigate the tracking performance of an adaptive STE, where $\mathbf{W}(k) = [\mathbf{w}_1(k) \ \mathbf{w}_2(k) \cdots \mathbf{w}_Q(k)]$ denotes the weight matrix of all the Q STEs. Since $J_{\text{MSE}}(\mathbf{w}_q(k), k)$ is a stochastic quantity, whose value depends on the channel

realisation, averaging over a number of different runs is necessary. Ultimately, the SER can be simulated to assess the equalisation performance.

3. Semi-blind GN-CMA+SDD algorithm

Let the number of available training symbols be K , and denote the available training data as

$$\begin{cases} \mathbf{X}_K = [\mathbf{x}(1) \ \mathbf{x}(2) \ \cdots \ \mathbf{x}(K)], \\ \bar{\mathbf{s}}_{K,q} = [s_q(1-\tau_q) \ s_q(2-\tau_q) \ \cdots \ s_q(K-\tau_q)]^T. \end{cases} \tag{16}$$

The LS estimate of the STE's weight vector based on $\{\mathbf{X}_K, \bar{\mathbf{s}}_{K,q}\}$ is readily given as

$$\mathbf{w}_q(0) = (\mathbf{X}_K \mathbf{X}_K^H)^{-1} \mathbf{X}_K \bar{\mathbf{s}}_{K,q}^* \tag{17}$$

In order to maintain throughput, the number of training pilots should be as small as possible. To ensure that $\mathbf{X}_K \mathbf{X}_K^H$ has a full rank, on the other hand, K should be chosen to be slightly larger than N_{STE} , the dimension of $\mathbf{x}(k)$. Because the training data with $K \approx N_{\text{STE}}$ are generally insufficient, the initial LS weight vector (17) may not be sufficiently accurate to open the eye. Therefore, decision direct adaptation is generally unsafe. Also directly applying the SG-CMA+SDD blind scheme of [31] to adapt the STE (12) with $\mathbf{w}_q(0)$ of Eq. (17) as the initial weight vector suffers from slow convergence and high steady-state MSE misadjustment, because $\mathbf{x}(k)$ is highly correlated. In the work [33], a GN-CMA+SDD algorithm was proposed to adjust the STE (12) with $\mathbf{w}_q(0)$ of Eq. (17) as the initial weight vector, which is capable of converging fast and accurately to the optimal MMSE STE solution under a stationary environment.

In the GN-CMA+SDD based STE [33], the STE's weight vector is split into two parts, yielding $\mathbf{w}_q(k) = \mathbf{w}_{q,c}(k) + \mathbf{w}_{q,d}(k)$. The initial $\mathbf{w}_{q,c}$ and $\mathbf{w}_{q,d}$ are simply set to $\mathbf{w}_{q,c}(0) = \mathbf{w}_{q,d}(0) = 0.5\mathbf{w}_q(0)$, where $\mathbf{w}_q(0)$ is given by the LS estimate of Eq. (17). A GN algorithm uses the inverse of the autocorrelation matrix of $\mathbf{x}(k)$ to modify the stochastic gradient [34,35]. Just like in the RLS algorithm, this inverse matrix can be updated recursively according to [21]

$$\mathbf{P}(k) = \lambda^{-1} \mathbf{P}(k-1) - \lambda^{-1} \mathbf{g}(k) \mathbf{x}^H(k) \mathbf{P}(k-1), \tag{18}$$

with

$$\mathbf{g}(k) = \frac{\lambda^{-1} \mathbf{P}(k-1) \mathbf{x}(k)}{1 + \lambda^{-1} \mathbf{x}^H(k) \mathbf{P}(k-1) \mathbf{x}(k)}, \tag{19}$$

where $0 < \lambda < 1$ is the forgetting factor [21]. The initial $\mathbf{P}(0)$ can be set to $\mathbf{P}(0) = (\mathbf{X}_K \mathbf{X}_K^H)^{-1}$.

The weight vector $\mathbf{w}_{q,c}$ is updated using the GN-CMA according to

$$\mathbf{w}_{q,c}(k+1) = \mathbf{w}_{q,c}(k) + \mu_{\text{CMA}} \mathbf{P}(k) \varepsilon^*(k) \mathbf{x}(k), \tag{20}$$

with

$$\varepsilon(k) = y_q(k) (\Delta - |y_q(k)|^2), \tag{21}$$

where $y_q(k) = \mathbf{w}_q^H(k) \mathbf{x}(k)$, $\Delta = E[|s_q(k)|^4] / E[|s_q(k)|^2]^2$ and μ_{CMA} is the step size of the CMA. This GN-CMA algorithm reduces to the conventional SG-CMA [38,39] if $\mathbf{P}(k)$ is replaced with an identity matrix. It is well-known that the step size for the SG-CMA must be chosen sufficiently small to avoid divergence, particularly in a highly correlated signal

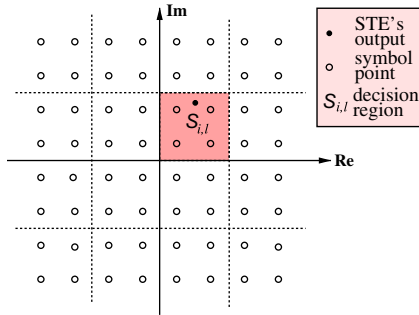


Fig. 3. Local decision region partition for soft decision-directed adaptation with 64-QAM constellation.

environment. By contrast, the step size of the GN-CMA algorithm can be set to a value much larger than the step size of the SG-CMA counterpart.

The weight vector $\mathbf{w}_{q,d}$ is updated using the GN-SDD scheme, which is now summarised. The complex phasor plane is divided into the $M/4$ rectangular regions, as illustrated in Fig. 3, and each region $\mathcal{S}_{i,l}$ contains four symbol points as defined by

$$\mathcal{S}_{i,l} = \{s_{r,m}, r = 2i-1, 2i, m = 2l-1, 2l\}, \tag{22}$$

where $1 \leq i, l \leq \sqrt{M}/2$. If the STE's output $y_q(k) \in \mathcal{S}_{i,l}$, a local approximation of the marginal probability density function (PDF) of $y_q(k)$ is given by [31,32]

$$\hat{p}(\mathbf{w}_q(k), y_q(k)) \approx \sum_{r=2i-1}^{2i} \sum_{m=2l-1}^{2l} \frac{1}{8\pi\rho} e^{-(|y_q(k)-s_{r,m}|^2/2\rho)}, \tag{23}$$

where ρ is the cluster width associated with the four clusters of each $\mathcal{S}_{i,l}$. The SDD scheme [31–33] is designed to maximise the local marginal PDF criterion

$$J_{\text{LMAP}}(\mathbf{w}_q(k), k) = \rho \log(\hat{p}(\mathbf{w}_q(k), y_q(k))). \tag{24}$$

In particular, the GN-SDD algorithm updates $\mathbf{w}_{q,d}$ according to

$$\mathbf{w}_{q,d}(k+1) = \mathbf{w}_{q,d}(k) + \mu_{\text{SDD}} \mathbf{P}(k) \frac{\partial J_{\text{LMAP}}(\mathbf{w}_q(k), k)}{\partial \mathbf{w}_{q,d}}, \tag{25}$$

where μ_{SDD} is the step size of the SDD, and

$$\frac{\partial J_{\text{LMAP}}(\mathbf{w}_q(k), k)}{\partial \mathbf{w}_{q,d}} = \frac{1}{Z_N} \sum_{r=2i-1}^{2i} \sum_{m=2l-1}^{2l} e^{-(|y_q(k)-s_{r,m}|^2/2\rho)} (s_{r,m} - y_q(k))^* \mathbf{x}(k), \tag{26}$$

with

$$Z_N = \sum_{r=2i-1}^{2i} \sum_{m=2l-1}^{2l} e^{-(|y_q(k)-s_{r,m}|^2/2\rho)}. \tag{27}$$

This GN-SDD algorithm reduces to the SG-SDD algorithm of [31,32] by replacing $\mathbf{P}(k)$ with an identity matrix. Note that, for the SG-SDD algorithm, the step size μ_{SDD} has significant influence on the performance of the algorithm, as too large value of μ_{SDD} results in divergence while too small value of μ_{SDD} leads to slow convergence. By contrast, for the GN-SDD algorithm, μ_{SDD} can be set to a much larger value than for the step size of the SG-SDD

counterpart. The performance of the GN-SDD algorithm is not overly sensitive to the cluster width ρ , defined in the context of the local PDF (23), as in the case of the SG-SDD [30–32].

It is interesting to point out that a more generic partition of the STE’s weight vector is

$$\mathbf{w}_q = \alpha \mathbf{w}_{q,c} + (1-\alpha) \mathbf{w}_{q,d}, \tag{28}$$

where $0 \leq \alpha \leq 1$. It is clear that $\alpha = 1$ corresponds to a pure CMA based STE while $\alpha = 0$ is related to a pure SDD based STE. Setting $\alpha = 0.5$ leads to the concurrent CMA+SDD based STE considered here. Depending on the channel condition, appropriate value of α may be chosen to yield a potentially better performance. However, this appropriate weighting value is difficult to find. In the absence of any *a priori* information, the weight vector partition of $\mathbf{w}_{q,c} = \mathbf{w}_{q,d} = 0.5 \mathbf{w}_q$ can be regarded as an optimal choice.

4. Simulation study

4.1. Stationary system

This example, taken from [40], was used to demonstrate that the semi-blind GN-CMA+SDD based STE was capable of converging fast to the optimal MMSE STE solution and its convergence speed was very close to that of the training-based RLS algorithm under a stationary dispersive MIMO environment. The system supported $Q=3$ users with $P=4$ receive antennas, and the modulation scheme was 16-QAM. The $P \cdot Q = 12$ constant CIRs $\mathbf{c}_{p,q}$, $1 \leq p \leq 4$ and $1 \leq q \leq 3$, can be found in [40], where each CIR had $n_C=3$ taps. The STE’s temporal filter order was chosen as $D=7$. The optimal decision delays were found to be $\tau_1 = 5$ for user one, $\tau_2 = 4$ for user two and $\tau_3 = 3$ for user three. These decision delays were used in the simulation. The average SER over all the $Q=3$ optimal MMSE STEs, depicted in Fig. 4, was used as the benchmark performance. For

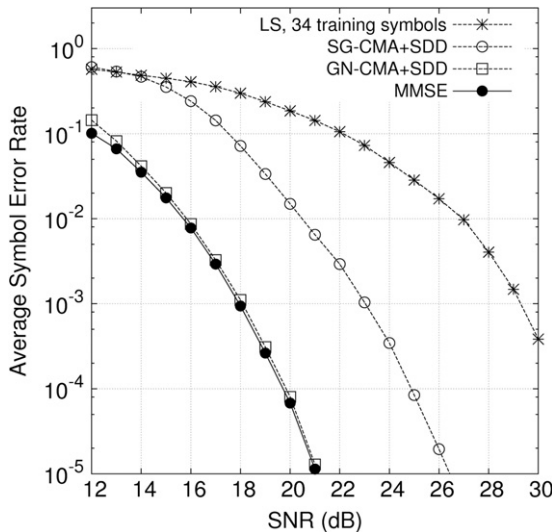


Fig. 4. Comparison of the average SER performance for the training-based LS STE with $K=34$ symbols as well as the semi-blind SG-CMA+SDD, semi-blind GN-CMA+SDD, and optimal MMSE STEs, for the stationary MIMO system.

this example, the STE’s dimension was $N_{STE} = 28$ and we chose $K=34$ for the initial training of a semi-blind STE. Given the $K=34$ training data, the LS estimate of the STE weight vector was provided by Eq. (17), and the average SER performance of this LS training-based STE is also depicted in Fig. 4, where it can be seen that $K=34$ was insufficient for the LS training based STE to achieve an adequate SER performance.

Because this was a stationary system, the forgetting factor was set to $\lambda = 1.0$ for both the training-based RLS and semi-blind GN-CMA+SDD based STEs. We also tested the semi-blind SG-CMA+SDD based STE [30] for a comparison. Given a SNR value, $K=34$ training pilots were first used to provide the initial weight vector of the STE according to (17). For all the $Q=3$ SG-CMA+SDD based STEs, $\mu_{CMA} = 0.00001$, $\mu_{SDD} = 0.0002$ and $\rho = 0.1$ were chosen, while $\mu_{CMA} = 0.01$, $\mu_{SDD} = 0.95$ and $\rho = 0.1$ were used for all the three GN-CMA+SDD based STEs. These parameters were found empirically to yield the best performance in terms of convergence speed and steady-state misadjustment. Fig. 5 plots the learning curve of the GN-CMA+SDD adaptive algorithm, in terms of the average MSE, in comparison with that obtained by the SG-CMA+SDD adaptive algorithm as well as the result obtained by the training-based RLS algorithm. It can be seen from Fig. 5 that the SG-CMA+SDD algorithm converged very slowly and was incapable of approaching the optimal MMSE STE solution due to an excessively high steady-state misadjustment, under a highly dispersive MIMO environment. By contrast, the GN-CMA+SDD algorithm was capable of converging fast and accurately to the MMSE STE solution. Next, given a range of SNR values, the average SER performance of the GN-CMA+SDD based and SG-CMA+SDD based semi-blind STEs after convergence were plotted in Fig. 4, in comparison with that of the optimal MMSE STE solution. The performance of the training-based RLS STE, not shown, was indistinguishable from the MMSE STE solution.

4.2. Non-stationary system

The system used in our simulation again supported $Q=3$ users with $P=4$ receive antennas, and the modulation scheme was 16-QAM. Each of the $P \cdot Q = 12$ CIRs had $n_C=3$ taps. The system was however under continuously fluctuating fading, leading to

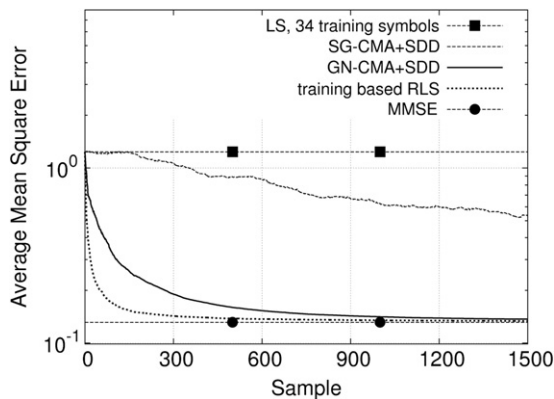


Fig. 5. Convergence performance of the SG-CMA+SDD, GN-CMA+SDD and training-based RLS STEs in terms of the average mean square error, given SNR of 19 dB and averaged over 20 runs, for the stationary MIMO system.

a different fading magnitude and phase for each CIR tap $c_{i,p,q}$ at each time instant k . The STE's temporal filter order was chosen as $D=5$. Note that there was a trade off in choosing an appropriate temporal filter length D . A larger D offered potentially a better

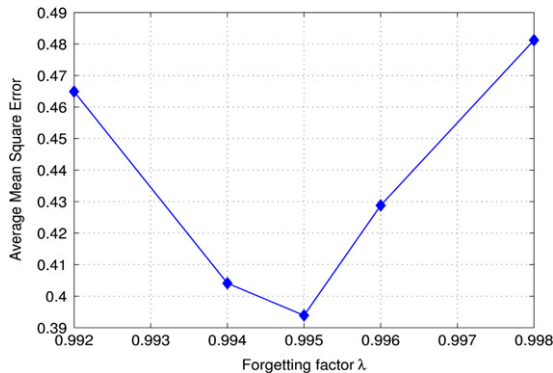


Fig. 6. Influence of the forgetting factor λ to the average MSE of the training-based RLS algorithm, given SNR of 20 dB and averaged over 50 runs, for the continuously fluctuating fading MIMO system with $f_d = 10^{-5}$.

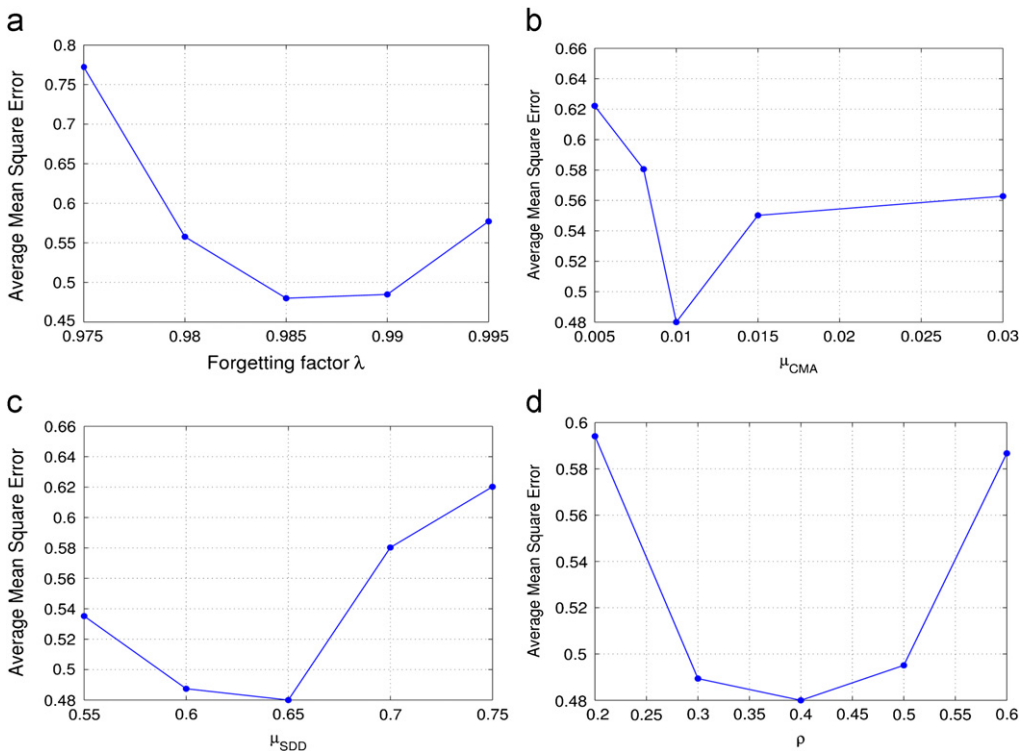


Fig. 7. Influence of (a) the forgetting factor λ with $\mu_{CMA} = 0.01$, $\mu_{SDD} = 0.65$ and $\rho = 0.4$, (b) the CMA step size μ_{CMA} with $\lambda = 0.985$, $\mu_{SDD} = 0.65$ and $\rho = 0.4$, (c) the SDD step size μ_{SDD} with $\lambda = 0.985$, $\mu_{CMA} = 0.01$ and $\rho = 0.4$, and (d) the cluster width ρ with $\lambda = 0.985$, $\mu_{CMA} = 0.01$ and $\mu_{SDD} = 0.65$, to the average MSE of the semi-blind GN-CMA+SDD algorithm, given SNR of 20 dB and averaged over 50 runs, for the continuously fluctuating fading MIMO system with $f_d = 10^{-5}$.

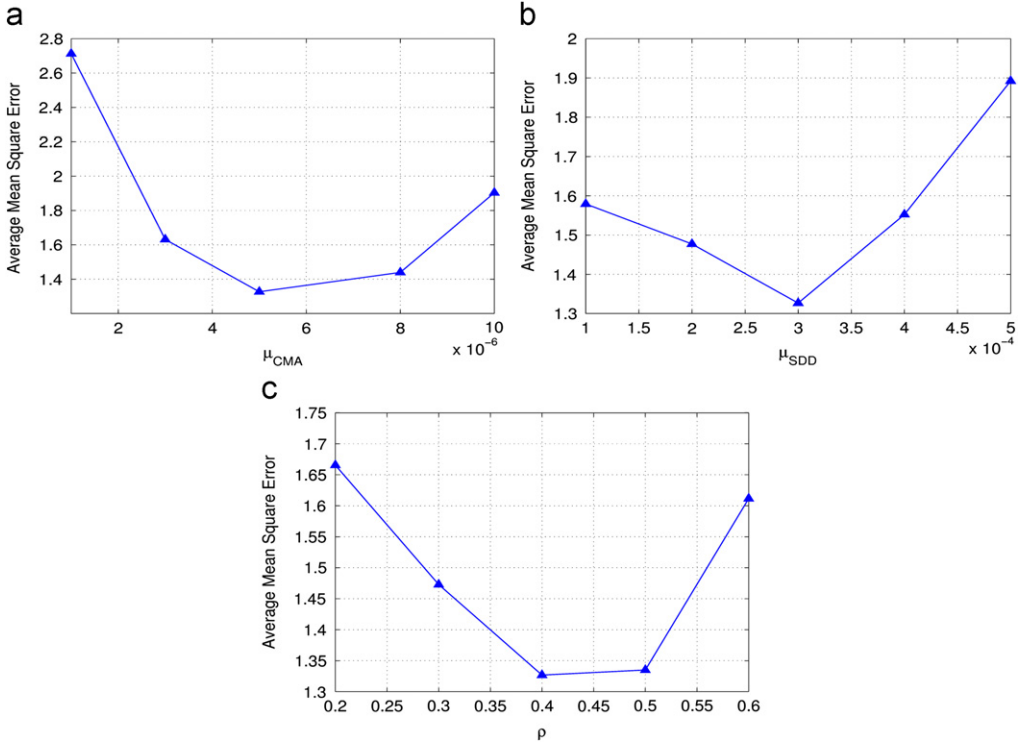


Fig. 8. Influence of (a) the CMA step size μ_{CMA} with $\mu_{SDD} = 3 \times 10^{-4}$ and $\rho = 0.4$, (b) the SDD step size μ_{SDD} with $\mu_{CMA} = 5 \times 10^{-6}$ and $\rho = 0.4$, and (c) the cluster width ρ with $\mu_{CMA} = 5 \times 10^{-6}$ and $\mu_{SDD} = 3 \times 10^{-4}$, to the average MSE of the semi-blind SG-CMA+SDD algorithm, given SNR of 20 dB and averaged over 50 runs, for the continuously fluctuating fading MIMO system with $f_d = 10^{-5}$.

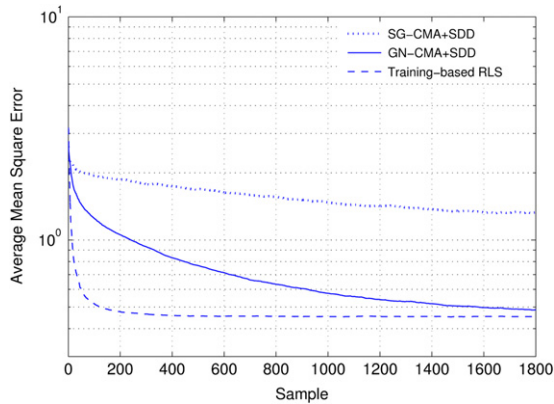


Fig. 9. Tracking performance comparison of the training-based RLS, semi-blind SG-CMA+SDD and semi-blind GN-CMA+SDD based STES, in terms of the average MSE, given SNR=20 dB and averaged over 50 runs, for the continuously fluctuating fading MIMO system with $f_d = 10^{-5}$.

performance but could result in a longer adaptation period and higher steady-state misadjustment, which was a particular problem for time-varying channels. The three decision delays of the three STEs were set to $\tau_1 = \tau_2 = \tau_3 = 2$. As the CIRs were changed at each k , the RLS based STE benchmark kept training continuously, which was obviously impractical to implement in reality but its performance offered a lower bound of the system’s achievable performance. For a semi-blind adaptive STE, the number of training symbols was $K=24$, which was slightly larger than the STE’s dimension of $N_{STE} = 20$.

We considered the fading system with the normalised Doppler frequency $f_d = 10^{-5}$. Given the SNR value of 20 dB, Fig. 6 plots the influence of the forgetting factor λ to the average MSE performance of the training-based RLS algorithm. The result of Fig. 6 suggests that the optimal forgetting factor for the training-based RLS STE was $\lambda = 0.995$. The procedure of choosing the algorithmic parameters of the GN-CMA+SDD algorithm was illustrated in Fig. 7, given the

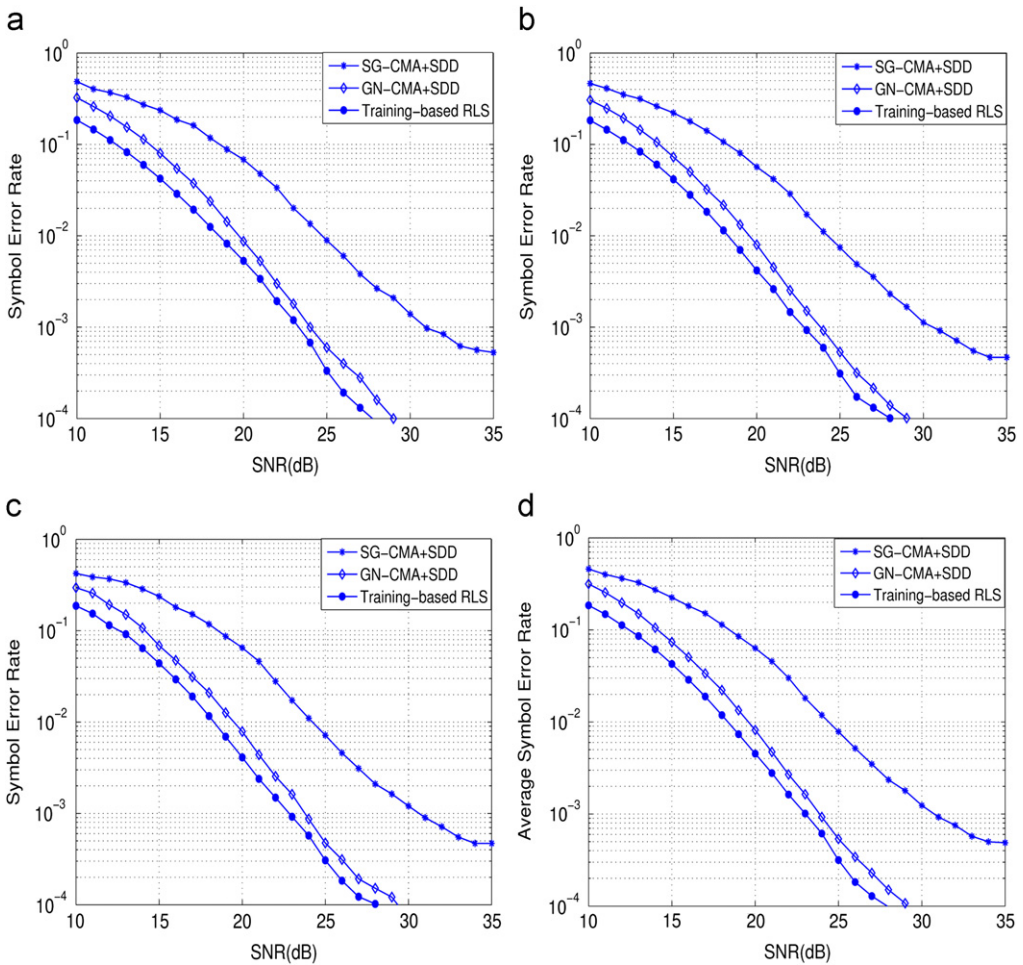


Fig. 10. SER performance comparison of the training-based RLS, semi-blind SG-CMA+SDD and semi-blind GN-CMA+SDD based STEs: (a) user one, (b) user two, (c) user three, and (d) average over all the three users, for the continuously fluctuating fading MIMO system with $f_d = 10^{-5}$.

SNR value of 20 dB, where it can be seen that appropriate algorithmic parameter values were the forgetting factor $\lambda = 0.985$, the CMA step size $\mu_{\text{CMA}} = 0.01$, the SDD step size $\mu_{\text{SDD}} = 0.65$ and the cluster width $\rho = 0.4$. Similarly, appropriate algorithmic parameters found empirically for the SG-CMA+SDD algorithm were the CMA step size $\mu_{\text{CMA}} = 5 \times 10^{-6}$, the SDD step size $\mu_{\text{SDD}} = 3 \times 10^{-4}$ and the cluster width $\rho = 0.4$, as confirmed in Fig. 8.

Fig. 9 plots the learning curves of the training-based RLS, semi-blind SG-CMA+SDD and semi-blind GN-CMA+SDD based STEs, in terms of the average MSE over all the $Q=3$ users, given the SNR value of 20 dB. It can be seen from Fig. 9 that the tracking performance of the semi-blind GN-CMA+SDD algorithm was close to that of the continuously training-based RLS algorithm. The result of Fig. 9 also confirms that the semi-blind SG-CMA+SDD algorithm suffered from slow convergence and excessively high steady-state misadjustment in the highly dispersive and fading MIMO signal environment. The SERs of the continuously training-based RLS, semi-blind SG-CMA+SDD and semi-blind GN-CMA+SDD based STEs are depicted in Fig. 10(a)–(c), for the users one to three, respectively, while the average SERs over all the three users for the three adaptive STEs are compared in Fig. 10 (d). The results obtained in Fig. 10 demonstrate that the SER performance of the semi-blind GN-CMA+SDD based STE was close to that of the continuously training-based RLS STE. This is very significant, considering the fact that the continuously training-based RLS STE is impossible to realise and its SER offers a low bound of the system’s achievable performance.

We next increases the normalised Doppler frequency to $f_d = 10^{-4}$, which represented a fast fading scenario. The three STEs had the same structure as in the case of $f_d = 10^{-5}$ and the number of the initial training symbols was again set to $K=24$. Fig. 11 depicts the learning curves of the training-based RLS, semi-blind SG-CMA+SDD and semi-blind GN-CMA+SDD based STEs, in terms of the average MSE over all the $Q=3$ users, given the SNR value of 20 dB. For the training-based RLS algorithm, the optimal forgetting factor was empirically found to be $\lambda = 0.993$. For the GN-CMA+SDD algorithm, appropriate algorithmic parameters were found to be $\lambda = 0.98$, $\mu_{\text{CMA}} = 0.01$, $\mu_{\text{SDD}} = 0.45$ and $\rho = 0.4$, while the algorithmic parameters of the SG-CMA+SDD algorithm were chosen empirically to be $\mu_{\text{CMA}} = 5 \times 10^{-6}$, $\mu_{\text{SDD}} = 0.0005$ and $\rho = 0.4$. From Fig. 11, it can

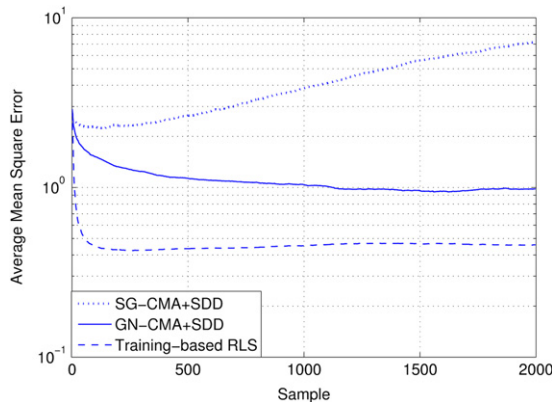


Fig. 11. Tracking performance comparison of the training-based RLS, semi-blind SG-CMA+SDD and semi-blind GN-CMA+SDD based STEs, in terms of the average MSE, given SNR=20 dB and averaged over 50 runs, for the continuously fluctuating fading MIMO system with $f_d = 10^{-4}$.

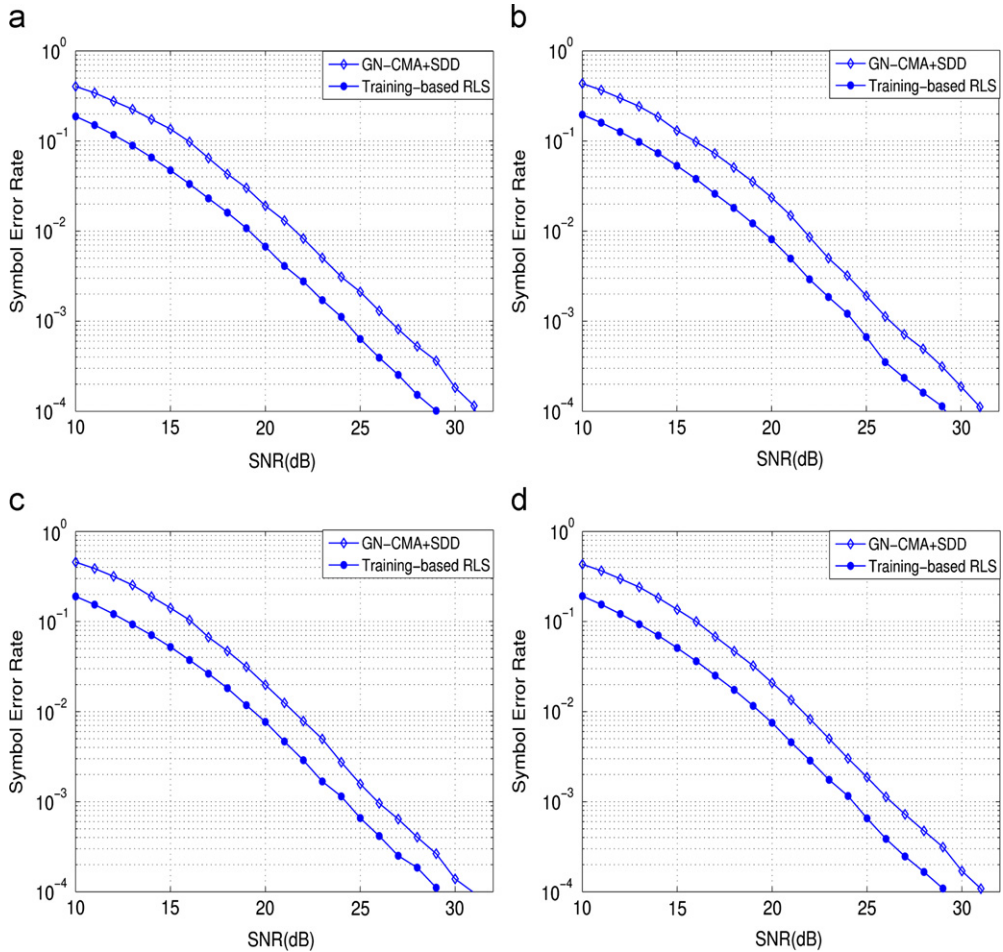


Fig. 12. SER performance comparison of the training-based RLS and semi-blind GN-CMA+SDD based STEs: (a) user one, (b) user two, (c) user three, and (d) average over all the three users, for the continuously fluctuating fading MIMO system with $f_d = 10^{-4}$.

be seen that the SG-CMA+SDD algorithm was incapable of tracking such a fast fading MIMO channel. By contrast, the GN-CMA+SDD algorithm was able to offer an adequate tracking performance under such a fast fading environment. This observation is further confirmed by the SER plots of Fig. 12(a)–(d).

5. Conclusions

A semi-blind STE based on a concurrent CMA and SDD adaptive algorithm has been investigated for frequency selective Rayleigh fading MIMO systems that employ high throughput QAM signalling. The scheme is semi-blind, as a minimum number of training symbols, approximately equal to the dimension of the STE, is used to provide a rough LS estimate of the STE weight vector for the initialisation. The concurrent GN-CMA+SDD

blind adaptive scheme is then adopted to adapt the STE. This semi-blind STE scheme has a complexity similar to that of the training-based RLS algorithm. Our simulation results involving a continuously fluctuating fading MIMO channel have demonstrated that the tracking performance of this semi-blind GN-CMA+SDD algorithm is close to that of the continuously training-based RLS algorithm. This confirms that the semi-blind adaptive GN-CMA+SDD based STE offers an effective and practical means to successfully operate under the highly dispersive and fading MIMO environment.

References

- [1] A.-J. van der Veen, S. Talwar, A. Paulraj, A subspace approach to blind space–time signal processing for wireless communication systems, *IEEE Transactions on Signal Processing* 45 (1) (1997) 173–190.
- [2] M. Martone, Complex scaled tangent rotations (CSTAR) for fast space–time adaptive equalization of wireless TDMA, *IEEE Transactions on Communications* 46 (12) (1998) 1587–1591.
- [3] A. Lozano, C. Papadias, Layered space–time receivers for frequency-selective wireless channels, *IEEE Transactions on Communications* 50 (1) (2002) 65–73.
- [4] D.P. Palomar, M.A. Lagunas, Joint transmit–receive space–time equalization in spatially correlated MIMO channels: a beamforming approach, *IEEE Journal on Selected Areas in Communications* 21 (5) (2003) 730–743.
- [5] R. Schober, S. Pasupathy, Noncoherent space–time equalization, *IEEE Transactions on Wireless Communications* 2 (3) (2003) 537–548.
- [6] X. Zhu, R.D. Murch, Layered space–time equalization for wireless MIMO systems, *IEEE Transactions on Wireless Communications* 2 (6) (2003) 1189–1203.
- [7] M. Koca, B.C. Levy, Turbo space–time equalization of TCM for broadband wireless channels, *IEEE Transactions on Wireless Communications* 3 (1) (2004) 50–59.
- [8] X. Zhu, R.D. Murch, Layered space–frequency equalization in a single-carrier MIMO system for frequency-selective channels, *IEEE Transactions on Wireless Communications* 3 (5) (2004) 701–708.
- [9] C.B. Papadias, Unsupervised receiver processing techniques for linear space–time equalization of wideband multiple input/multiple output channels, *IEEE Transactions on Signal Processing* 52 (2) (2004) 472–482.
- [10] V. Zarzoso, A.K. Nandi, Exploiting non-Gaussianity in blind identification and equalisation of MIMO FIR channels, *IEE Proceedings Vision, Image & Signal Processing* 151 (1) (2004) 69–75.
- [11] A. Wolfgang, S. Chen, L. Hanzo, Radial basis function network assisted space–time equalisation for dispersive fading environments, *Electronics Letters* 40 (16) (2004) 1006–1007.
- [12] C. Luschi, B. Mulgrew, Estimation of the output error statistics of space–time equalization in an antenna array EGPRS receiver with soft-decision decoding, *IEEE Transactions on Wireless Communications* 4 (4) (2005) 1377–1382.
- [13] S. Chen, A. Livingstone, L. Hanzo, Minimum bite-error rate design for space–time equalization-based multiuser detection, *IEEE Transactions on Communications* 54 (5) (2006) 824–832.
- [14] S. Chen, L. Hanzo, A. Livingstone, MBER space–time decision feedback equalization assisted multiuser detection for multiple antenna aided SDMA systems, *IEEE Transactions on Signal Processing* 54 (8) (2006) 3090–3098.
- [15] A. Wolfgang, S. Chen, L. Hanzo, Parallel interference cancellation based turbo space–time equalization in the SDMA uplink, *IEEE Transactions on Wireless Communications* 6 (2) (2007) 609–616.
- [16] A. Wolfgang, J. Akhtman, S. Chen, L. Hanzo, Reduced-complexity near-maximum-likelihood detection for decision feedback assisted space–time equalization, *IEEE Transactions on Wireless Communications* 6 (7) (2007) 2407–2411.
- [17] T. Ait-Idir, S. Saoudi, N. Naja, Spacetime turbo equalization with successive interference cancellation for frequency-selective MIMO channels, *IEEE Transactions on Vehicular Technology* 57 (5) (2008) 2766–2778.
- [18] Y. Lee, W.-R. Wu, Adaptive decision feedback space–time equalization with generalized sidelobe cancellation, *IEEE Transactions on Vehicular Technology* 57 (5) (2008) 2894–2906.
- [19] L. Hanzo, S.X. Ng, T. Keller, W. Webb, *Quadrature Amplitude Modulation: From Basics to Adaptive Trellis-Coded, Turbo-Equalised and Space–Time Coded OFDM, CDMA and MC-CDMA Systems*, John Wiley and IEEE Press, Chichester, UK, 2004.

- [20] IEEE 802.16, Air Interface for Fixed Broadband Wireless Access System, Section 8. PHY, 2004.
- [21] S. Haykin, Adaptive Filter Theory, second ed., Prentice-Hall, Upper Saddle River, NJ, 1996.
- [22] L. Tang, R.W. Liu, V.C. Soon, Y.F. Huang, Indeterminacy and identifiability of blind identification, *IEEE Transactions on Circuits and Systems* 38 (5) (1991) 499–509.
- [23] Y. Inouye, R.W. Liu, A system-theoretic foundation for blind equalization of an FIR MIMO channel system, *IEEE Transactions on Circuits and Systems Part I: Fundamental Theory and Applications* 49 (4) (2002) 425–436.
- [24] A. Medles, D.T.M. Slock, Semiblind channel estimation for MIMO spatial multiplexing systems, in: *Proceedings of VTC2001-Fall*, vol. 2, Atlantic City, NJ, October 7–11, 2001, pp. 1240–1244.
- [25] C. Cozzo, B.L. Hughes, Joint channel estimation and data detection in space–time communications, *IEEE Transactions on Communications* 51 (8) (2003) 1266–1270.
- [26] T. Wo, P.A. Hoeher, A. Scherb, K.D. Kammeyer, Performance analysis of maximum-likelihood semiblind estimation of MIMO channels, in: *Proceedings of VTC2006-Spring*, vol. 4, Melbourne, Australia, May 7–10, 2006, pp. 1738–1742.
- [27] A.K. Jagannatham, B.D. Rao, Whiteness-rotation-based semi-blind MIMO channel estimation, *IEEE Transactions on Signal Processing* 54 (3) (2006) 861–869.
- [28] Z. Ding, T. Ratnarajah, C.F.N. Cowan, HOS-based semi-blind spatial equalization for MIMO Rayleigh fading channels, *IEEE Transactions on Signal Processing* 56 (1) (2008) 248–255.
- [29] M. Abuthinien, S. Chen, L. Hanzo, Semi-blind joint maximum likelihood channel estimation and data detection for MIMO systems, *IEEE Signal Processing Letters* 15 (2008) 202–205.
- [30] S. Chen, W. Yao, L. Hanzo, Semi-blind adaptive spatial equalisation for MIMO systems with high-order QAM signalling, *IEEE Transactions on Wireless Communications* 7 (11) (2008) 4486–4491.
- [31] S. Chen, E.S. Chng, Concurrent constant modulus algorithm and soft decision directed scheme for fractionally-spaced blind equalization, in: *Proceedings of ICC 2004*, vol. 4, Paris, France, June 20–24, 2004, pp. 2342–2346.
- [32] S. Chen, T.B. Cook, L.C. Anderson, A comparative study of two blind FIR equalizers, *Digital Signal Processing* 14 (1) (2004) 18–36.
- [33] S. Chen, L. Hanzo, Fast converging semi-blind space–time equalisation for dispersive QAM MIMO systems, *IEEE Transactions on Wireless Communications* 8 (8) (2009) 3969–3974.
- [34] P.S.R. Diniz, Adaptive Filtering: Algorithms and Practical Implementation, second ed., Kluwer Academic Publishers, Boston, MA, 2003.
- [35] R.C. de Lamare, R. Sampaio-Neto, Adaptive MBER decision feedback multiuser receivers in frequency selective fading channels, *IEEE Communications Letters* 7 (2) (2003) 73–75.
- [36] A. Paulraj, R. Nabar, D. Gore, Introduction to Space–Time Wireless Communications, Cambridge University Press, Cambridge, UK, 2003.
- [37] D. Tse, P. Viswanath, Fundamentals of Wireless Communication, Cambridge University Press, Cambridge, UK, 2005.
- [38] D. Godard, Self-recovering equalization and carrier tracking in two-dimensional data communication systems, *IEEE Transactions on Communications COM-28* (11) (1980) 1867–1875.
- [39] J.R. Treichler, B.G. Agee, A new approach to multipath correction of constant modulus signals, *IEEE Transactions on Acoustics, Speech and Signal Processing ASSP-31* (2) (1983) 459–472.
- [40] S. Chen, L. Hanzo, H.-T. Cheng, Semi-blind gradient-Newton CMA and SDD algorithm for MIMO space–time equalisation, in: *Proceedings of Globecom 2009*, Honolulu, Hawaii, 5 pages, 30 November–4 December, 2009.